Polycyclic Aromatic Hydrocarbons Generated by the Incomplete Combustion: Case of Fluoranthene

Siham Naima Derrar[1], Mostefa Belhakem[2]

***Abstract*—**Incipient soot nanoparticles represent a real threat, due to the fatal and irreversible damages they can cause on health and environment. The incomplete combustion of engine's fuel leads to the creation of these nanoparticles. It has been shown that they are formed by some extremely carcinogenic Polycyclic Aromatic Hydrocarbons (PAH), precisely, the aggregation of dimers and trimers and so on of PAH. Understanding the structural parameters of these aggregations is crucial to clarify the real composition of soot which remains not completely understood. This present paper is devoted to the study of the dimerization of fluoranthene. Different structural building ways have been suggested, with full and partial covering between the monomer entities. The number of the interacting six membered rings varies between one and three cycles, from each monomer. The impact of structure on both binding energy and equilibrium distance has been analyzed. Binding energies vary between -5.88 and -8.41 kcal/mol. The structural parameters seem to play a key role in the dispersion-type interactions for the fluoranthene dimers.

***Keywords*—**Fluoranthene, Polycyclic Aromatic Hydrocarbon, Stacking dimers, Soot.

I. Introduction

NOWADAYS, emission from industrial processes as well as the number of cars, air traffic and shipping boats with combustion engines, is steadily increasing [1-6]. Despite the fact that a huge effort is being devoted to develop electromobility, combustion engines fueled by either diesel or gasoline is still prevailing.

Incomplete combustion generates nanoparticles known as soot particles. These latter are introduced as Polycyclic Aromatic Hydrocarbons (PAH). They are considered to be the most common pollutants in our environment [7-11]. In fact, their presence in air, soil, water, food, etc, represent a real danger on the public health along with ecology. A very close relationship between PAH presence in the ambient air and the potential to contribute to human cancer has been already pointed out [12].

PAH molecules consist of two or more fused aromatic rings. They are essentially constituted by carbon and hydrogen atoms. About 500 types of PAH have been detected in air, many of them display carcinogenic properties.

Even though many experimental studies have been achieved on soot nanoparticles, their formation is still poorly understood [13-19]. The development of the incipient soot nanoparticles has been described as a random agglomerate of dimers and trimers of PAHs [20-23].

In this optic, we decided to carry out a theoretical study on one of the most important PAHs: fluoranthene ($C_{16}H_{10}$). This molecule has been admitted as one of the prior PAHs in ambient air which can cause serious damages on health. Hence, dimerization of stacking fluoranthene has been undertaken in this study. Indeed, several stacking structures have been considered in order to detect any kind of influence on the binding energy and the equilibrium distance.

II. Calculation details

Full geometry optimization of fluoranthene monomer has been done without symmetry constraints at MP2/6-311G(d,p) level of theory. Starting from the final geometry, the corresponding stacking dimers of the molecules have been constructed. We choose two types to build stacking structures: the first way is the Full Parallel Sandwich (FPS) dimer (Fig. 1) and the second one is the Partial Parallel Sandwich (PPS) dimer. In the PPS structures, each monomer contributes either with one or two interacting cycles (Fig. 2).

For each structure, the intermolecular separation interval has been included between 3.4Å and 4.1Å. Then, a set of single-points calculations have been completed at the intermolecular distances above-cited. To deal with basis set superposition error, we used the counterpoise method [24]. All results have been fitted to a Morse potential in order to extract the equilibrium distance and the corresponding binding energy. For the dispersion energy, we used B-97D [25] method associated to cc-PVTZ [26] basis set. Calculations have been performed with Gaussian03 program package [27].

Siham Naima Derrar[1] is with Laboratoire de Structure, Elaboration et Application des Matériaux Moléculaires, Mostaganem University, 27000 Algeria and with the Department of Pharmacy, Faculty of Medecine, Djilali Liabès University, Sidi Bel Abbès 22000 Algeria (e-mail: derrarsiham@yahoo.fr).

Mostefa Belhakem[2], is with Laboratoire de Structure, Elaboration et Application des Matériaux Moléculaires, Mostaganem University, 27000 Algeria (e-mail: mbelhakem@hotmail.com).

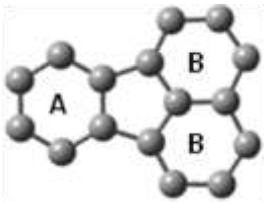

Fig. 1 Structure of fluoranthene monomer and FPS fluoranthene dimer (Ball and stick model with hided hydrogen atoms)

III. Results and Discussion

The structures of PPS dimers are regrouped in Fig. 2. In these structures the number of the six membered interacting cycles is less than in the FPS structure. The corresponding binding energy of each structure has been calculated upon the plots that show the equilibrium distance (Fig. 3). Results are collected in Table I.

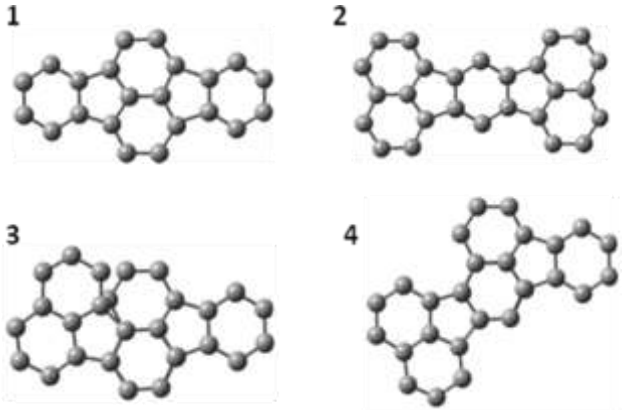

Fig. 2 Top view of PPS fluoranthene dimers (1 with two interacting cycles while 2, 3 and 4 with one interacting cycle, from each monomer)

The equilibrium distance values vary from 3.5 to 3.7 Å through one to three interacting cycles. Within the same interacting cycle's number, binding energy differs from -5.88 to -7.96 kcal/mol, in PPS2, PPS3 and PPS4. Binding energy of PPS1 exceeds that one of FPS though the first one detains more interacting cycle's number (Table I). This indicates that the π-π interactions type existing in these dimers do not quantitatively influence the strength of the binding energy.

TABLE I
INTERACTING CYCLE'S NUMBER FROM EACH MONOMER, BINDING ENERGIES, DIPOLE MOMENT AND HOMO-LUMO ENERGY GAP

	Int. Cyc	Class	R_e	$E_{Binding}$	μ	ΔE_{H-L}
FPS	03	A/A, B/B	3.7	-8.31	0.624	0.082
PPS1	02	B/B	3.6	-8.41	0.013	0.085
PPS2	01	A/A	3.5	-5.88	0.001	0.092
PPS3	01	A/B	3.5	-7.96	0.731	0.089
PPS4	01	A/B	3.5	-7.30	0.657	0.093

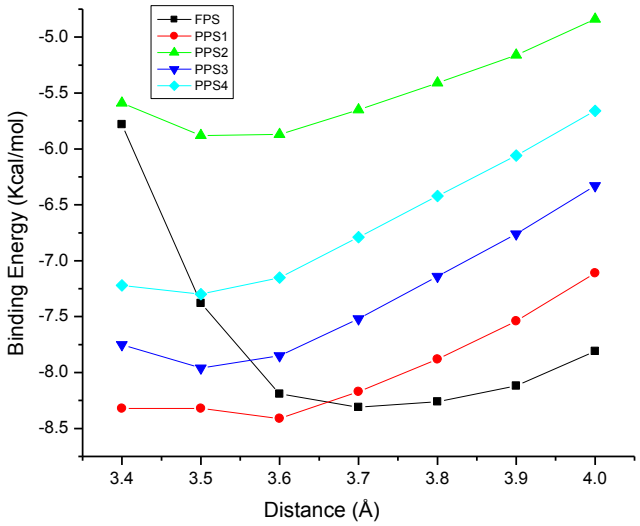

Fig. 3 Potential energy curves of FPS and PPS structures versus intermolecular distances

The Six membered rings of fluoranthene have been labeled as A and B types as shown in Fig. 1. Three classes of dimers are distinguished upon the intermolecular interaction they present. The first class is assumed to B/B interacting cycles; the second one is assigned to A/B and the last one to A/A class.

As expected, the first class of dimer, where two cycles from each monomer are interacting exhibits the strongest binding energy.

For the PPS structures 2, 3 and 4 where interaction involves one cycle from each monomer, we notice two categories: A/B with the strongest binding energies and A/A with the smallest one (Table I). This indicates again that interaction energy seems to be governed by the nature of the cycles that interact with each other. Thus, binding energy decreases in the order of: B/B>A/B>A/A.

For each dimer studied, we report dipole moment and HOMO-LUMO energy gap recorded at the equilibrium geometry (Table I).

The smallest dipole moment and the smallest binding energy match together, for PPS2. No link has been found between μ and the binding energies (Fig. 4-a).

HOMO-LUMO energy gap is a good indicator of stability; the larger the gap the greater the stability of the molecule. Results show that the most stable system is the PPS4 dimer. It also coincides with the highest dipole moment magnitude. no accurate rule has been found with binding energy, nonetheless, the smallest values match with the dimers possessing the highest interacting cycle's number FPS and PPS1 (Fig. 4-b).

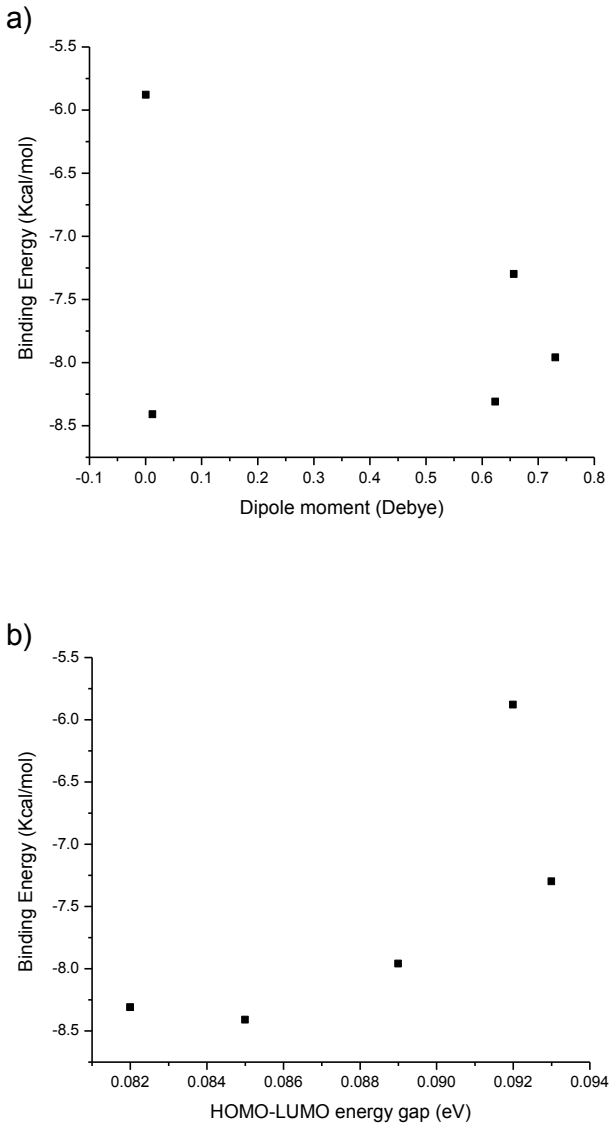

Fig. 4 Equilibrium binding energy versus: a) dipole moment and b) HOMO-LUMO energy gap

IV. Conclusion

Nowadays, it is noteworthy to elucidate the composition of soot nanoparticles due to the huge impact they have on public health and ecology. Soot nanoparticles are mainly formed during the incomplete combustion in engines and are primarily constituted by aggregation of Polycyclic Aromatic Hydrocarbons (PAH).

In this paper, we have focused on the basic non-alternant PAH: fluoranthene. This PAH is assumed to be one of the most pollutant and carcinogenic in the environment.

Several stacking dimers have been analyzed, where the monomers interact in a full and a partial parallel positions, respectively.

The corresponding binding energy and the intermolecular equilibrium distance for each dimer studied have been investigated.

Equilibrium distance varies upon the number of interacting cycles from 3.5 to 3.7Å.

A fluctuation of binding energy from -5.88 to -8.41 kcal/mol has been recorded through all the dimers. When one cycle from each monomer is interacting, the binding energy differs from -5.88 to -7.96 kcal/mol.

We also could find a relation between the type of the interacting cycles and the binding energies and we established a suitable classification.

For this kind of dimers, the structural properties and the way in which the monomers interact with each other are a key issue to basically understand the soot nanoparticles formation.

References

[1] A. Stampfl, M. Maier, R. Radykewicz, P. Reitmeir, M. Gött-Licher, R. Niessner, "Langendorff heart: a model system to study cardiovascular effects of engineered nanoparticles)," ACS Nano, vol. 5, no 7, pp. 5345-5353, 2011.

[2] B. Franck, M. Schuster, R. Schlögl, D. Su, "Emission aktivierter Rußpartikel: die Kehrseite der Medaille moderner Dieselmotoren," Ang. Res., vol. 125, no 10, pp. 2736-2741, 2013.

[3] T. H. Fletcher, M. S. Solum, D. C. Grant, S. Critchfield, R. J. Pugmire, "Solid state ^{13}C and ^{1}H NMR studies of the evolution of the chemical structure of coal char and tar during devolatilization," Proc. Combustion Institute, vol. 23, no 1, pp 1231-1237, 1991.

[4] M. J. Wornat, A. F. Sarofim, J. P. Longwell, "Changes in the degree of substitution of polycyclic aromatic compounds from pyrolysis of a high-volatile bituminous coal," Energy Fuels, vol 1, pp 431-437, 1987.

[5] M. J. Wornat, A. F. Sarofim, J. P. Longwell, "Pyrolysis-induced changes in the ring number composition of polycyclic aromatic compounds from a high-volatile bituminous coal," Proc. Combustion Institute, vol. 22, no 1, pp 135-143, 1989.

[6] M. A. Serio, D. G. Hamblen, J. R. Markham, P. R. Solomon, "Kinetics of volatile products evolution in coal pyrolysis: experiment and theory," Energy fuels, vol. 1, no 2, pp 138-152, 1987.

[7] IARC (1983). "Polynuclear aromatic compounds, Part 1, Chemical, environmental and experimental data," IARC Monogr. Eval. Carcinog. Risk Chem. Hum, vol 32, pp 1-453.

[8] IARC (1984). "Polynuclear aromatic compounds, Part 2, carbon blacks, mineral oils (lubrifiant base oils and derived products) and some niroarenes," IARC Monogr. Eval. Carcinog. Risk Chem. Hum, vol 33, pp 1-222.

[9] IARC (1984). "Polynuclear aromatic compounds, Part 3, Industrial exposures in aluminium production, coal gasification, coke production, and iron and steel founding," IARC Monogr. Eval. Carcinog. Risk Chem. Hum, vol 34, pp 1-219.

[10] IARC (1985). "Polynuclear aromatic compounds, Part 4, bitumens, coal-tars and derived products, shale-oils and soots," IARC Monogr. Eval. Carcinog. Risk Chem. Hum, vol. 35, pp 1-247.

[11] IARC (2010). "Some non-heterocyclic polycyclic aromatic hydrocarbons and some related exposures," IARC Monogr. Eval. Carcinog. Risk . Hum, vol. 92, pp 1-853.

[12] A. Dipple, R. C. Moschel, C. A. H. Bigger, "Polynuclear aromatic carcinogens," In Chemical Carinogens, 2nd ed.; C. E. Searle, Ed.; ACS Monograph 182; Am. Chem. Soc. Vol. 1, pp 41-164, 1984.

[13] M. Balthasar, M. Fraft, "A stochastic approach to solve the particle size distribution function of soot particles in laminar premixed ethylene flames," Combust. Flame, vol. 133, pp. 289-298, 2003.

[14] R. I. A. Patterson, J. Singh, M. Balthasar, M. Kraft, W. Wagner "Extending stochastic soot simulation to higher pressures," Combust. Flame, vol. 145, no 3, pp. 638-642, 2006.

[15] R. I. A. Patterson, J. Singh, M. Balthasar, M. Kraft, J. Norris, "The linear process deferment algorithm: a new technique for solving population balance equations," SIAM J. Comput., vol. 28, pp. 303-320, 2006.

[16] J. Singh, R. I. A. Patterson, M. Kraft, H. Wang, "Numerical simulation and sensitivity analysis of detailed soot particle size distribution in

laminar premixed ethylene flames," Combust. Flame, vol. 145, pp. 117-127, 2006.
[17] M. S. Celnik, R. I. A. Patterson, M. Kraft, W. Wagner, "Coupling of stochastic soot population balance to gas-phase chemistry using operator splitting," Combust. Flame, vol. 148, no 3, pp. 158-176, 2007.
[18] M. S. Celnik, A. Raj, R. H. West, R. I. A. Patterson, M. Kraft, "An aromatic site description of soot particles," Combust. Flame, vol. 155, no 1-2, pp. 161-180, 2008.
[19] M. S. Celnik, M. Sander, A. Raj, R. H. West, M. Kraft, "Modelling soot formation in a premixed flame using an aromatic-site soot model and improved oxidation rate," Proc. Combust. Inst., vol. 32, no 1, pp. 639-646, 2009.
[20] M. Balthasar, M. Frenklach, "Monte-Carlo simulation of soot particle coagulation and aggregation: The effect of a realistic size distribution," Proc. Combust. Inst., vol. 30, pp. 1467-1475, 2005.
[21] A. Kazakov, M. Frenklach "Dynamic modeling of soot particle coagulation and aggregation: Implementation with the method of moments and application to high-pressure laminar premixed flames," Combust. Flame, vol. 114, pp. 484-501, 1998.
[22] R. I. A. Patterson, M. Kraft, "Models for the aggregate structure of soot particles," Combust. Flame, vol. 151, pp. 160-172, 2007.
[23] N. Morgan, M. Kraft, M. Balthasar, D. Wong, M. Frenklach, P. Mitchell, "Numerical simulations of soot aggregation in premixed laminar flames," Proc. Combust. Inst., vol. 31, no 1, pp. 693-700, 2007.
[24] S. F. Boys, F. Bernardi, "The calculation of small molecular interactions by the differences of separate total energies. Some procedures with reduced errors," Mol. Phys. 19 (1970) 553-566
[25] S. Grimme, "Semiempirical GGA-type density functional constructed with a long-range dispersion correction," J. Comput. Chem. 27 (2006) 1787-1799
[26] T. H. Jr Dunning, "Gaussian basis sets for use in correlated molecular calculations. I. The atoms boron through neon and hydrogen," J. Chem. Phys. 90 (1989) 1007-1023.
[27] M. J. Frisch, G. W. Trucks *et al*. Gaussian03, Revision E. 01, Gaussian. Inc., Wallingford, CT, 2004.